Polymer Chemistry

Radical-Radical Coupling Effects in the Direct-Growth Grafting-Through Synthesis of Bottlebrush Polymers using RAFT and ROMP

Journal:	*Polymer Chemistry*
Manuscript ID	PY-ART-06-2022-000794.R1
Article Type:	Paper
Date Submitted by the Author:	11-Sep-2022
Complete List of Authors:	Alaboalirat, Mohammed; Virginia Tech, Chemistry Vu, Clark; Virginia Tech, Chemistry Matson, John; Virginia Tech, Chemistry

ARTICLE

Radical-Radical Coupling Effects in the Direct-Growth Grafting-Through Synthesis of Bottlebrush Polymers using RAFT and ROMP

Mohammed Alaboalirat, Clark Vu, and John B. Matson*

Received 00th January 20xx,
Accepted 00th January 20xx

DOI: 10.1039/x0xx00000x

The direct-growth technique was used to synthesize several macromonomers (MMs) employing reversible addition-fragmentation chain transfer (RAFT) polymerization by growing directly from a norbornene-functionalized chain transfer agent (CTA). We aimed to investigate the formation of bisnorbornenyl species resulting from radical termination by combination (i.e., coupling) during RAFT polymerization at different monomer conversion values in four types of monomers: styrene, *tert*-butyl acrylate, methyl methacrylate and *N*-acryloyl morpholine. Ring-opening metathesis polymerization (ROMP) of these MMs using Grubbs 3rd generation catalyst (G3) at an MM:G3 ratio of 100:1 resulted in the formation of bottlebrush polymers. Analysis by size-exclusion chromatography (SEC) revealed high molar mass shoulders of varying intensities attributed to the incorporation of these bisnorbornenyl species to generate dimeric or higher-order bottlebrush polymer oligomers. The monomer type in the RAFT step heavily influenced the amount of these bottlebrush polymer dimers and oligomers, as did the monomer conversion value in the RAFT step: We found that the ROMP of polystyrene MMs with a target backbone degree of polymerization of 100 produced detectable coupling at ≥20% monomer conversion in the RAFT step, while it took ≥80% monomer conversion to observe coupling in the poly(*tert*-butyl acrylate) MMs. We did not detect coupling in the poly(methyl methacrylate) MMs, but broadening of the SEC peaks and an increase in dispersity occurred, suggesting the presence of metathesis-active alkene-containing chain ends created by disproportionation. Finally, poly(*N*-acryloyl morpholine) MMs, even when reaching 90% monomer conversion in the RAFT step, showed no detectable coupling in the bottlebrush polymers. These results highlight the importance of monomer choice and RAFT polymerization conditions in making MMs for ROMP grafting-through to make well-defined bottlebrush polymers.

Introduction

Ring-opening metathesis polymerization (ROMP) of macromonomers (MMs) has become a reliable approach for generating bottlebrush polymers with a high density of side chains attached to the backbone.[1-3] Termed the grafting-through approach, this method typically relies on the synthesis of a norbornene-containing MM made commonly by a ring-opening polymerization (ROP) or reversible-deactivation radical polymerization (RDRP) technique. In a second step, the highly active Grubbs 3rd generation catalyst (G3) is routinely applied to initiate the synthesis of bottlebrush polymers via ROMP. The grafting-through ROMP strategy ensures perfect grafting density on each repeat unit while providing excellent control of both the side chain and backbone degrees of polymerization (N_{sc} and N_{bb}, respectively).[4-6] However, obtaining well-defined bottlebrush polymers with high MM to bottlebrush conversions, monomodal molar mass distributions, and low dispersities depends heavily on the purity of the MM used in the ROMP reaction.[7, 8]

While many types of impurities in MMs can cause problems in ROMP, it is critical to limit the amount of termination in the preceding RDRP reaction because termination by combination forms a bisnorbornenyl species. In the ROMP step, bisnorbornenyl species lead to bottlebrush polymers linked to other bottlebrush polymers, i.e., bottlebrush dimers or oligomers.[9] For example, high molar mass shoulders or bimodal molar mass distributions in the SEC traces of the resultant bottlebrush polymers have been observed in several investigations, particularly when the MMs were prepared using RDRP techniques such as atom-transfer radical polymerization (ATRP) or reversible addition–fragmentation chain transfer (RAFT) polymerization.[10-12] This concept is depicted graphically in **Figure 1**. Bisnorbornenyl species can also form even when radical polymerizations are not employed in the MM synthesis; for example, the diol impurity present in commercial monofunctionalized polyethylene glycol (PEG) can affect the synthesis of bottlebrush polymers.[13] Thus, synthetic methods to reduce the presence of bisnorbornenyl species in MMs are needed to achieve well-defined bottlebrush polymers, which are under investigation for the synthesis of complex polymer topologies[14-18] and applications including biomedicine,[19-25] electronic and transport materials,[26, 27] elastomers,[6, 28-32] photonic crystals,[33-37] and nanoporous materials.[38-41]

Department of Chemistry and , Macromolecules Innovation Institute, 1040 Drillfield Dr., Blacksburg, VA 24061, USA.
E-mail: jbmatson@vt.edu
Electronic Supplementary Information (ESI) available: See DOI: 10.1039/x0xx00000x

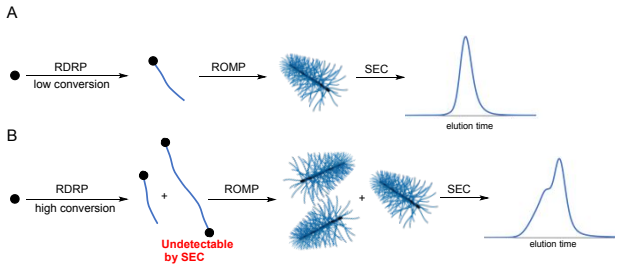

Figure 1. Schematic illustration of the effect of stopping the RDRP reaction in the MM synthesis at low (A) and high (B) MM to bottlebrush polymer conversion on the presence of bisnorbornenyl species and the control of bottlebrush polymer synthesis.

Two approaches are typically used to synthesize MMs monofunctionalized with a norbornene. One is the growth-then-coupling approach, which involves the coupling of the norbornene after the preparation of the MM, usually on the ω-end of the polymer. This approach eliminates the possibility of creating bisnorbornenyl species, but it lengthens the preparation of MMs.[9, 42] The second approach is the direct-growth approach, in which the norbornene group is attached to an initiator or RDRP chain transfer agent (CTA) before the preparation of the MM. Using this method, RDRP reactions are often run to a low monomer conversion to limit the production of the bisnorbornenyl species as shown by several research groups.[5, 43-48] The possibility for incorporation of the norbornene unit in an RDRP copolymerization must also be considered.[49]

Herein, we aimed to compare the amounts of bisnorbornenyl species formed in RAFT polymerizations mediated by norbornene-functionalized CTAs at various MM to bottlebrush polymer conversion values in four monomers from different classes commonly used to prepare bottlebrush polymers: styrene (S), *tert*-butyl acrylate (*t*BA), methyl methacrylate (MMA), and *N*-acryloyl morpholine (ACMO). The purpose of this study was to determine at what monomer conversion (in the RAFT step) the production of bisnorbornenyl species leads to a rapid increase in the dispersity of the bottlebrush polymer (in the ROMP step) when utilizing the direct-growth approach. Ideally, these results will serve as a reference to determine optimal MM to bottlebrush polymer conversion targets when using RDRP reactions for each MM monomer class.

Experimental Section

Materials

All reagents were obtained from commercial vendors and used as received unless otherwise stated. Solvents were obtained from solvent drying columns and used without further purification. Styrene, *tert*-butyl acrylate, methyl methacrylate, and *N*-acryloyl morpholine (ACMO) were passed through a small column of basic alumina to remove the radical inhibitor before use in polymerizations. G3 was prepared from Grubbs 2nd generation catalyst (G2) according to literature procedures and used within two days of its preparation.[50, 51] The preparation of norbornene alcohol **1** was as reported previously.[44]

Characterization

NMR spectra were measured on Bruker 500 MHz or Agilent 400 MHz spectrometers. ^{1}H and ^{13}C NMR chemical shifts are reported in ppm relative to internal solvent resonances of $CDCl_3$. Yields refer to spectroscopically and chromatographically pure compounds unless otherwise stated. Size exclusion chromatography (SEC) was carried out in tetrahydrofuran (THF) containing BHT at 1 mL min^{-1} at 30 °C on two MIXED-B Agilent PLgel 10 µm columns connected in series with a Wyatt Optilab Rex refractive index detector (RI) and a Wyatt Dawn Heleos 2 light scattering (LS) detector. Specific refractive index increments (d*n*/d*c* values) used for MMs and bottlebrush polymers were 0.185 (PS),[52] 0.049 (PtBA, determined via offline measurements, Figure S65), 0.084 (PMMA),[52] and 0.105 (PACMO determined via offline measurements, Figure S66). A Biotage Selekt flash purification system was used for automated silica gel column purification using Biotage® Sfär Duo 5g columns. The mobile phase had a flow rate of 18 mL/min, and fractions were collected in 16 x 150 mm test tubes. Solvent systems for the purification of MMs were determined initially using TLC with UV visualization to observe the elution of the MMs; monomers were not easily visible by TLC. We used this information to set up a solvent gradient assuming the monomers would elute before the MMs, which we confirmed occurred in all cases by injecting monomers onto the Biotage system and determining their elution time under the chosen gradient.

Peak Deconvolution

The deconvolution of peaks in the SEC traces was carried out by adapting a published procedure using Multiple Peak Fit in OriginPro 2018.[53] In brief, overlapping peaks were deconvoluted by assuming a Gaussian distribution, yielding the relative areas of high- and low-molar mass peaks. The percentage of coupled bottlebrush product was calculated using the following equation:

$$P_{coupling} = \frac{A_1}{A_1 + A_2} \times 100\% \qquad \text{(Eq. 1)}$$

Where $P_{coupling}$ is the weight percentage of coupled bottlebrush polymer products. Also, A_1 and A_2 are the relative areas of the high and low molar mass peaks, respectively.

Synthesis of Norbornene-Functionalized Trithiocarbonate 2

Norbornene-functionalized trithiocarbonate **2** was synthesized based on a literature procedure.[44] NMR spectra were consistent with reported results. ^{1}H NMR ($CDCl_3$): δ 6.07 (m, 2H), 4.22 (d, 1H), 3.95 (t, 1H), 3.27 (t, 2H), 2.82 (s, 1H), 2.66 (s, 1H), 1.70 (s, 6H), 1.31 (m, 3H), 1.25 (m, 20H), 0.88 (t, 3H). ^{13}C NMR ($CDCl_3$): δ 221.6, 173.2, 137.0, 136.5, 70.2, 56.2, 45.1, 43.8, 41.8, 37.9, 37.0, 32.1, 29.8, 29.7, 29.6, 29.5, 29.3, 29.1, 28.1, 25.6, 25.6, 22.9, 14.3.

Synthesis of Norbornene-Functionalized Trithiocarbonate 3

Norbornene-functionalized trithiocarbonate **3** was synthesized based on adaptations of literature procedures (**Scheme 1**).[4, 54, 55] First, a small single crystal of iodine and magnesium turnings (2.45 g, 100 mmol) were added to a 300 mL roundbottom flask with dry THF (40 mL). Another solution was made by dissolving bromobenzene (15.7 g, 100 mmol) in THF (40 mL). This bromobenzene solution was added dropwise to the I_2/Mg suspension at rt using an addition funnel at a slow rate over a period of 30 min to avoid a rapid temperature increase of the Grignard solution. Stirring continued for 3 h until the Mg was consumed. The Grignard solution flask was then put in an ice bath, allowed to cool for 30 min, and then carbon disulfide (7.6 g, 100 mmol) was added dropwise via syringe over a period of 5 min. The solution became red as the roundbottom flask warmed slowly in the ice bath. The reaction was allowed to stir in the ice bath for 30 min, and then it was stirred for 1 h at rt. The roundbottom flask was placed again in an ice bath and allowed to cool down for 30 min. Next, a solution that contained *p*-tosyl chloride (9.5 g, 50 mmol) in THF (50 mL) was added dropwise using an addition funnel over a period of 10 min. The color of the solution changed from red to purple at this stage. Reaction progress was monitored by TLC (10% ethyl acetate (EtOAc) in hexanes), indicating the complete disappearance of bromobenzene after 1 h. Solvents were removed via rotary evaporation, and the crude product mixture was loaded onto a silica column that was eluted at 10% EtOAc in hexanes to obtain bis(thiobenzoyl) disulfide as purple powder (4.1 g, 27% yield). ^{1}H NMR ($CDCl_3$): δ 8.09 (d, *J* = 8.6 Hz, 4H), 7.61 (m, 2H), 7.45 (m, 4H) and ^{13}C NMR ($CDCl_3$): δ 219.8, 143.9, 133.3, 128.8, 127.8. The ^{1}H and ^{13}C NMR spectra matched previously published reports.[55]

Next, 4,4'-azobis(4-cyanopentanoic acid) (4.7 g, 17 mmol) and bis(thiobenzoyl) disulfide (3.4 g, 11 mmol) were dissolved in THF (40 mL) in a 250 mL Schlenk tube. The solution was bubbled with N_2 for 15 min and then placed in an oil bath at 80 °C for 18 h. The Schlenk tube was removed from the oil bath and allowed to cool for 30 min and then opened to air. The contents were transferred to a roundbottom flask, then the mixture was concentrated via rotary evaporation. The crude product was dissolved in CH_2Cl_2 and then dry loaded onto silica for purification using a silica column. The product was isolated using 20% EtOAc in hexanes as the eluent. The product, 4-cyano-4-(phenylcarbonothioylthio)pentanoic acid, was isolated as red powder (2.0 g, 33% yield). ^{1}H NMR ($CDCl_3$): δ 7.92 (m, 2H), 7.57 (m, 1H), 7.40 (m, 2H), 2.79-2.40 (m, 4H), 1.94 (s, 3H) and ^{13}C NMR ($CDCl_3$): δ 222.8, 177.4, 145.3, 133.6, 129.0, 127.3, 119.1, 46.2, 33.5, 29.9 24.9. The ^{1}H and ^{13}C NMR spectra matched previously published reports.[56]

Finally, in a roundbottom flask equipped with a stir bar, *exo*-5-norbornene-2-methanol (0.70 g, 5.64 mmol), 4-cyano-4-(phenylcarbonothioylthio)pentanoic acid (1.57 g, 5.64 mmol), and 4-(dimethylamino)pyridine (0.344 g, 2.82 mmol) were dissolved in dry CH_2Cl_2 (40 mL). While stirring, 1-ethyl-3-(3-dimethylaminopropyl) carbodiimide (EDC) (1.62 g, 8.46 mmol) was added to the mixture as a solid. The reaction mixture was stirred for 16 h, after which the 4-cyano-4-(phenylcarbonothioylthio)pentanoic acid had been completely consumed based on TLC (10% EtOAc in hexanes, UV visualization). The reaction mixture was concentrated in vacuo and purified using silica gel flash chromatography with EtOAc/hexanes as the eluting solvent (1:10). The product was obtained as a red oil (1.2 g, 55% yield).^{1}H NMR ($CDCl_3$): δ 7.9 (m, 2H), 7.55 (m, 1H), 7.39 (m, 2H), 6.09 (m, 2H), 4.18 (dd, *J* = 7 and 11 Hz, 1H), 4.00 (dd, *J* = 9 and 11 Hz, 1H), 2.84 (s, 1H), 2.76-2.65 (m, 3H), 2.65-2.54 (m, 1H), 2.49-2.40 (m, 1H) 1.94 (s, 1H), 1.73 (m, 1H), 1.39-1.22 (m, 4H), 1.15 (m, 1H).^{13}C NMR ($CDCl_3$): δ 222.3, 171.6, 144.6, 137.0, 136.2, 133.1, 128.6, 125.7, 118.6, 69.3, 45.8, 45.0, 43.7, 41.6, 38.0, 33.5, 29.9, 29.6, 24.2. The ^{1}H and ^{13}C NMR spectra matched previously published reports.[4]

Synthesis of Polystyrene Macromonomers (PS-MMs)

A typical styrene polymerization procedure with a 20% monomer conversion is as follows: Norbornene-functionalized trithiocarbonate **2** (0.025 g, 0.053 mmol), styrene (0.74 mL, 6.5 mmol), DMF (1.04 mL) and AIBN (0.44 mg, 0.0027 mmol) (using a stock solution of 1 mg/mL AIBN in DMF) were added to a 100 mL Schlenk tube equipped with a stir bar. The mixture in the Schlenk tube was deoxygenated by 3 freeze-pump-thaw cycles and then backfilled with N_2. The reaction mixture was submerged in an oil bath at 90 °C for ca. 4 h. Aliquots were collected throughout the reaction via N_2-purged syringe and analyzed via ^{1}H NMR spectroscopy to ensure that ~20% conversion had been reached. Once the targeted conversion was reached, the reaction was terminated by removing the Schlenk tube from the oil bath and exposing the contents of the Schlenk tube to air by removing the Kontes valve. The resultant PS-MM was purified by loading the solvent mixture onto a Biotage silica column. The monomer and MM absorbed strongly at a wavelength of 200 nm, which was used to monitor the eluents during the elution of the column. The solvent gradient started from 100% hexanes to 40% EtOAc in hexanes; residual monomer eluted first at 5% EtOAc in hexanes, and the PS-MM eluted from 30-35% EtOAc in hexanes. PS-MM fractions were collected, and the solvent was removed via rotary evaporation in a roundbottom flask. The PS-MM was dissolved in a CH_2Cl_2 (10 mL) and was transferred to a tared 20 mL glass vial. The CH_2Cl_2 was removed through air drying initially and was followed by drying under vacuum in a Schlenk line overnight. The dried PS-MM (100 mg) was analyzed by SEC (M_n = 2.8 kg/mol, Đ = 1.10). The molar ratios of reagents for the RAFT reaction were [styrene]/[CTA **2**]/[AIBN] = 244:1:0.05 when targeting 10% conversion, [styrene]/[CTA **2**]/[AIBN] = 122:1:0.05 when targeting 20% conversion, [styrene]/[CTA **2**]/[AIBN] = 81:1:0.05 when targeting 30% conversion, [styrene]/[CTA **2**]/[AIBN] = 61:1:0.05 when targeting 40% conversion and [styrene]/[CTA **2**]/[AIBN] = 49:1:0.05 when targeting 50% conversion. In all cases, the DMF/styrene volume ratio was kept at 2:1.

Synthesis of Poly(*tert*-Butyl Acrylate) Macromonomers (P*t*BA-MMs)

A typical *t*BA polymerization procedure with a 50% monomer conversion is as follows: Norbornene-functionalized trithiocarbonate **2** (0.050 g, 106 µmol), *t*BA (0.62 mL, 4.25 mmol), DMF (1.6 mL) and AIBN (0.872 mg, 5.31 µmol) (using a stock solution of 1 mg/mL AIBN in DMF) were added to a 100 mL Schlenk tube equipped with a stir bar. The mixture in the Schlenk tube was deoxygenated by 3 freeze-pump-thaw cycles and then backfilled with N_2. The reaction mixture was submerged in an oil bath at 70 °C for ca. 2 h. Aliquots were collected throughout the reaction via N_2-purged syringe and analyzed via ^{1}H NMR spectroscopy to ensure that ~50% conversion had been reached. Once the targeted conversion was reached, the reaction was terminated by removing the Schlenk tube from the oil bath and exposing the contents of the Schlenk tube to air by removing the Kontes valve. The resultant P*t*BA-MM was purified by loading the solvent mixture onto a Biotage silica column. The monomer and MM both absorbed strongly at wavelengths of 265 nm and 305 nm, respectively. These values were used to monitor the eluents during the elution of the column. The solvent gradient started from 100% hexanes to 100% EtOAc; the residual monomer eluted first at 10% EtOAc in hexanes, and the P*t*BA-MM eluted from 17-20% EtOAc in hexanes. P*t*BA-MM fractions were collected, and the solvent was removed via rotary evaporation in a roundbottom flask. The P*t*BA-MM was dissolved in CH_2Cl_2 (10 mL) and transferred to a tared 20 mL glass vial. The CH_2Cl_2 was removed through air drying initially and was followed by drying under vacuum in a Schlenk line overnight. The dried P*t*BA-MM (110 mg) was analyzed by SEC (M_n = 2.9 kg/mol, Đ = 1.14). The molar ratios of reagents for the RAFT reaction were [*t*BA]/[CTA **2**]/[AIBN] = 39:1:0.05 when targeting 50% conversion, [*t*BA]/[CTA **2**]/[AIBN] = 32:1:0.05 when targeting 60% conversion, [*t*BA]/[CTA **2**]/[AIBN] = 28:1:0.05 when targeting 70% conversion, [*t*BA]/[CTA **2**]/[AIBN] = 24:1:0.05 when targeting 80% conversion and [*t*BA]/[CTA **2**]/[AIBN] = 22:1:0.05 when targeting 90% conversion. In all cases, the DMF/*t*BA volume ratio was kept at 4:1.

Synthesis of Poly(Methyl Methacrylate) Macromonomers (PMMA-MMs)

A typical MMA polymerization procedure with a 70% monomer conversion is as follows: Norbornene-functionalized trithiocarbonate **3** (0.030 g, 78 µmol), MMA (0.25 mL, 2.96 mmol), toluene (0.5 mL) and AIBN (1.28 mg, 7.78 µmol) (using a stock solution of 1 mg/mL AIBN in toluene) were added to a 100 mL Schlenk tube equipped with a stir bar. The mixture in the Schlenk tube was deoxygenated by 3 freeze-pump-thaw cycles and then backfilled with N_2. The reaction mixture was submerged in an oil bath at 70 °C for ca. 5 h. Aliquots were collected throughout the reaction via N_2-purged syringe and analyzed via ^{1}H NMR spectroscopy to ensure that ~70% conversion had been reached. Once the targeted conversion was reached, the reaction was terminated by removing the Schlenk tube from the oil bath and exposing the contents of the Schlenk tube to air by removing the Kontes valve. The resultant PMMA-MM was purified by loading the solvent mixture onto a Biotage silica column. The monomer and MM absorbed strongly at wavelengths of 253 nm and 330 nm, respectively. These values were used to monitor the eluents during the elution of the column. The solvent gradient started from 100% hexanes to 100% EtOAc; residual monomer eluted first from 40-65% EtOAc in hexanes, and the PMMA-MM eluted at 100% EtOAc. PMMA-MM fractions were collected, and the solvent was removed via rotary evaporation in a roundbottom flask. The PMMA-MM was dissolved in CH_2Cl_2 (10 mL) and transferred to a tared 20 mL glass vial. The CH_2Cl_2 was removed through air drying initially and was followed by drying under vacuum in a Schlenk line overnight. The dried PMMA-MM (50 mg) was analyzed by SEC (M_n = 3.1 kg/mol, Đ = 1.14). The molar ratios of reagents for the RAFT reaction were [MMA]/[CTA **3**]/[AIBN] = 52:1:0.1 when targeting 50% conversion, [MMA]/[CTA **3**]/[AIBN] = 43:1:0.1 when targeting 60% conversion, [MMA]/[CTA **3**]/[AIBN] = 37:1:0.1 when targeting 70% conversion, [MMA]/[CTA **3**]/[AIBN] = 32:1:0.1 when targeting 80% conversion and [MMA]/[CTA **3**]/[AIBN] = 29:1:0.1 when targeting 90% conversion. In all cases, the toluene/MMA volume ratio was kept at 7:1.

Synthesis of Poly(*N*-Acryloylmorpholine) Macromonomers (PACMO-MMs)

A typical ACMO polymerization procedure with a 60% monomer conversion is as follows: Norbornene-functionalized trithiocarbonate **2** (0.050 g, 106 µmol), ACMO (0.40 mL, 3.19 mmol), DMF (1.6 mL) and AIBN (0.872 mg, 5.31 µmol) (using a stock solution of 1 mg/mL AIBN in DMF) were added to a 100 mL Schlenk tube equipped with a stir bar. The mixture in the Schlenk tube was deoxygenated by 3 freeze-pump-thaw cycles and then backfilled with N_2. The reaction mixture was submerged in an oil bath at 70 °C for ca. 2 h. Aliquots were collected throughout the reaction via N_2-purged syringe and analyzed via ^{1}H NMR spectroscopy to ensure that ~60% conversion had been reached. Once the targeted conversion was reached, the reaction was terminated by removing the Schlenk tube from the oil bath and exposing the contents to air by removing the Kontes valve. The resultant PACMO-MM was purified by loading the solvent mixture directly onto a Biotage silica column. The monomer and MM absorbed strongly at a wavelength of 210 nm, which was used to monitor the eluents during the elution of the column. The solvent gradient started from 100% THF to 60% methanol in THF; DMF and residual ACMO monomer eluted at 100% THF, and the PACMO-MM started to elute from 30–40% MeOH in THF. The PACMO-MM fractions were collected, and the solvent was removed via rotary evaporation in a roundbottom flask. The PACMO-MM was dissolved in CH_2Cl_2 (10 mL) and transferred to a tared 20 mL glass vial. The CH_2Cl_2 was removed through air drying initially and was followed by drying under vacuum in a Schlenk line overnight. The dried PACMO-MM (120 mg) was analyzed by SEC (M_n = 3.0 kg/mol, Đ = 1.14). The molar ratios of reagents for the RAFT reaction were [ACMO]/[CTA **2**]/[AIBN] = 35.5:1:0.05

when targeting 50% conversion, [ACMO]/[CTA **2**]/[AIBN] = 30:1:0.05 when targeting 60% conversion, [ACMO]/[CTA **2**]/[AIBN] = 26:1:0.05 when targeting 70% conversion, [ACMO]/[CTA **2**]/[AIBN] = 22:1:0.05 when targeting 80% conversion and [ACMO]/[CTA **2**]/[AIBN] = 19:1:0.05 when targeting 90% conversion. In all cases, the DMF/ACMO volume ratio was kept at 6:1.

Synthesis of Bottlebrush Polymers via ROMP

A typical synthesis procedure for a bottlebrush polymer is as follows: MM A$^{60\%}$ (10.0 mg, 3.1 kg/mol, 3.2 µmol) was dissolved in CH_2Cl_2 (0.1 mL) in a vial equipped with a small stir bar. This vial was placed on a stir plate and allowed to stir at 400 rpm. In a second vial, G3 (2.4 mg, 3.3 µmol) was dissolved in CH_2Cl_2 (3.1 mL) to create a G3 stock solution. Next, 30 µL of the G3 stock solution was added rapidly to the first vial via a 100 µL syringe. The polymerization reaction mixture was allowed to stir for 60 min. The polymerization reaction was then terminated by adding 0.1 mL of ethyl vinyl ether. The reaction mixture was air-dried, and the residue was dissolved in THF to obtain an SEC trace. This procedure afforded bottlebrush polymer $A_{100}^{60\%}$; the other bottlebrush polymers were synthesized using the same procedure by varying the identity of the MM while maintaining an MM:G3 ratio of 100:1.

Results and Discussion

Macromonomer Synthesis

We first set out to prepare a total of 20 MMs, five from each monomer class with different % monomer conversion values. All MMs were synthesized starting from norbornene alcohol **1**, and this ROMP-active compound was coupled to two different RAFT CTAs. First, DMPA and norbornene alcohol **1** were coupled using EDC, which produced norbornene-functionalized trithiocarbonate **2** (**Scheme 1**), suitable for acrylamides, acrylates, and styrenics. The second CTA was prepared by coupling 4-cyano-4-(phenylcarbonothioylthio) pentanoic acid and norbornene alcohol **1** using EDC to produce trithiocarbonate **3**, suitable for methacrylates.

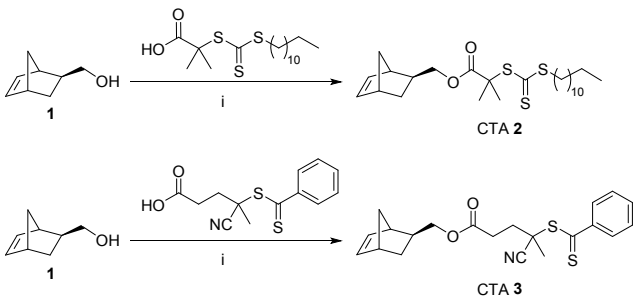

Scheme 1. Synthesis of norbornene-functionalized CTAs. Conditions: (i) EDC, DMAP, CH_2Cl_2, rt, 16 h.

For this study, we aimed to prepare MMs in the range of 3–4 kg/mol because MMs at this molar mass range typically undergo ROMP to produce bottlebrush polymers with ~95% conversion or higher.[4, 57, 58] Four different monomer types were used in RAFT polymerization to prepare four types of norbornene-functionalized MMs: PS, P*t*BA, PMMA, and PACMO. The general formula to represent the MMs is $X^{y\%}$, where *X* represents the type of monomer used (S for PS, T for P*t*BA, M for PMMA and A for PACMO), and *y*% represents the percentage of monomer conversion to polymer targeted in the RAFT polymerization. For example, **A$^{60\%}$** represents PACMO-MM with a targeted molar mass of 3–4 kg/mol and 60% monomer to PACMO-MM conversion in the RAFT step.

PS-MMs were synthesized starting with trithiocarbonate **2** under typical RAFT conditions (**Scheme 2A**). The targeted monomer conversions for PS-MMs were 10%, 20%, 30%, 40% and 50% (as PS has a high rate of termination by combination[59, 60]) while targeting 3–4 kg/mol. While three precipitations in MeOH were used in other reports to purify PS-MMs to eliminate unreacted styrene,[44] we used automated column chromatography with conventional silica to separate the monomer from the PS-MMs (**Figure S7**). The purity of the PS-MMs was confirmed by ^{1}H NMR spectroscopy, which revealed no olefin peaks (**Figure S8**). SEC traces (Figure S6) showed monomodal peaks with no signs of shouldering in either the RI or LS traces, and molecular weights by SEC and ^{1}H NMR spectroscopic end group analysis (Figures S45-49) were all very close to the expected values (Table 1, Table S1).

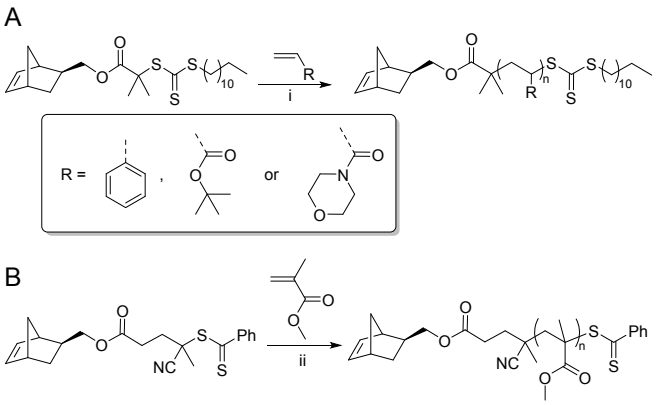

Scheme 2. Synthesis of (A) PS-MMs, P*t*BA-MMs, PACMO-MMs and (B) PMMA-MMs. Conditions: (i) PS-MM: DMF, AIBN, 90 °C, 4 h. P*t*BA-MM: DMF, AIBN, 70 °C, 5 h. PACMO-MM: DMF, AIBN, 70 °C, 2 h. (ii) PMMA-MM: Toluene, AIBN, 70 °C, 5 h.

P*t*BA-MMs were made starting with trithiocarbonate **2** under standard RAFT conditions, as shown in **Scheme 2A**. The targeted conversions for P*t*BA-MMs were 50%, 60%, 70%, 80% and 90% while targeting 3–4 kg/mol. As with the other monomers besides MMA, the ROMP reaction can be terminated if the unreacted *t*BA monomer is not completely removed. While purification of P*t*BA-MMs has been described using precipitation in 20% water in MeOH or hexanes at -60 °C,[61] we again separated residual *t*BA monomer from the P*t*BA-MMs using automated chromatography methods (**Figure S19**). The purity of all P*t*BA-MMs was confirmed by ^{1}H NMR spectroscopy, which revealed no monomer peaks (**Figure S20**).

Interestingly, unlike in the PS-MM traces, SEC analysis (Figure S18) of the P*t*BA-MMs revealed molar mass values somewhat larger than the expected 3–4 kg/mol (Table 1, Table S1) with high molar mass shoulders of increasing intensity with increasing conversion in the RAFT polymerization. For some of the MMs, the high molar mass shoulders cetainly contain small amounts bisnorbornenyl species either through radical-radical coupling reactions (or in the case of acrylates cross-termination with RAFT adduct radicals[62]) as confirmed below in the context of polymerization of these MMs. However, in the case of acrylates such as *t*BA, shoulders can also arise due to two other factors: 1) Branching during propagation, which occurs in all radical polymerizations of acrylates due to chain transfer to polymer;[63] and 2) Copolymerization with norbornene units, creating MMs with one or a few branch points. Keddie and coworkers recently showed in a detailed study that in copolymerizations of norbornenes with acrylates, more branch points arise with increasing conversion.[12] In sum, we attribute the increase in M_n measured by SEC and the increasing area of the high molar mass shoulders with increasing conversion in the PtBA-MMs to these four types of side reactions (coupling by termination, coupling by cross-termination, branching during propagation, and copolymerization). ROMP of these MMs, discussed below, suggests that coupling reactions only begin to contribute substantially to the shoulders at monomer conversions of 80% of greater.

We used trithiocarbonate **3** to make the PMMA-MMs based on previous reports from Wooley and coworkers in their syntheses of bottlebrush PMMA.[4] PMMA-MMs were synthesized under typical RAFT conditions, as shown in **Scheme 2B**. The targeted monomer conversions for PMMA-MMs were 50%, 60%, 70%, 80% and 90% while targeting 3–4 kg/mol. Again, we used automated column chromatography to purify the MMs (**Figure S29**). Because MMA is a type-IV olefin for Grubbs's catalysts,[64] it does not interfere with ROMP, but we removed it to be consistent with the other procedures. The purity of PMMA-MMs was verified by ^{1}H NMR spectroscopy, where no olefin peaks were observed (**Figure S30**). SEC traces showed molar masses close to expected values with monomodal peaks (Figure S28) and no significant shoulders, presumably because copolymerization of norbornenes is less favorable with methacrylates than with acrylates. M_n values by NMR end group analysis (Figures S55-59) were close to expected values and those measured by SEC (Table 1, Table S1).

Finally, starting from trithiocarbonate **2,** PACMO-MMs were synthesized under typical RAFT conditions (**Scheme 2A**). The monomer conversions for PACMO-MMs were 50%, 60%, 70%, 80% and 90%, with ratios of reagents adjusted to target a 3–4 kg/mol. Removal of unreacted ACMO monomer is vital as it can terminate the ROMP reaction. While PACMO-MMs were purified in previous reports by precipitating into ethyl ether three times,[44] we used automated column chromatography in this case as well (**Figure S37**). The purity of all PACMO-MMs was verified by ^{1}H NMR spectroscopy, where no olefin peaks were observed (**Figure S38**). SEC traces (Figure S36) showed slight high molecular weight shoulders in MMs **A$^{60\%}$** and **A$^{70\%}$** but not in the others. End group analysis (Figures S60-64) by ^{1}H NMR spectroscopy showed higher than expected molecular weights in these two MMs, suggesting a small amount of copolymerization, similar to the PtBA-MMs (Table 1, Table S1).

Table 1. MM names and SEC characterization data.

MM [a]	$M_{n,theo}$ [b] (kg/mol)	$M_{n,SEC}$ [c] (kg/mol)	$Đ$ [c]	MM [a]	$M_{n,theo}$ [b] (kg/mol)	$M_{n,SEC}$ [c] (kg/mol)	$Đ$ [c]
S$^{10\%}$	3.0	3.0	1.09	**M$^{50\%}$**	3.0	2.8	1.10
S$^{20\%}$	2.9	2.8	1.10	**M$^{60\%}$**	3.1	3.0	1.16
S$^{30\%}$	3.0	2.8	1.09	**M$^{70\%}$**	2.8	2.8	1.10
S$^{40\%}$	3.0	2.8	1.09	**M$^{80\%}$**	2.9	2.8	1.09
S$^{50\%}$	3.0	3.0	1.12	**M$^{90\%}$**	2.8	3.4	1.13
T$^{50\%}$	3.1	4.7	1.04	**A$^{50\%}$**	2.9	3.9	1.10
T$^{60\%}$	2.9	4.7	1.07	**A$^{60\%}$**	3.0	4.3	1.14
T$^{70\%}$	3.1	3.9	1.08	**A$^{70\%}$**	3.0	4.5	1.11
T$^{80\%}$	2.9	6.0	1.10	**A$^{80\%}$**	2.9	4.2	1.04
T$^{90\%}$	2.9	6.7	1.16	**A$^{90\%}$**	2.9	4.3	1.09

[a]Targeted molar mass of each MM is represented by $X^{y\%}$ where *X* is the MM type (S = PS, T = P*t*BA, M = PMMA and A = PACMO) and *y*% is the targeted monomer conversion percentage in the RAFT polymerization. [b]Expected (theoretical) M_n value based on an assumption of linear molar mass growth with monomer conversion, where monomer conversion was monitored using ^{1}H NMR spectroscopy. [c]Measured by SEC in THF at 30 °C using light scattering and refractive index detectors using d*n*/d*c* values noted in the Experimental Section.

Bottlebrush Polymer Synthesis

While the preparation of MMs by growth-then-coupling may eliminate the termination by combination problems in the bottlebrush polymer synthesis that occur when using the direct-growth method, many polymer chemists prefer direct-growth because it is a more straightforward synthetic approach that does not rely on quantitative end-group modification reactions. In this study, we aimed to use the direct-growth approach for each type of monomer to determine at what monomer conversion percentage during the RAFT polymerization we start to detect coupling or increased dispersity in the bottlebrush polymer formed in the ROMP grafting-through step. High molar mass shoulders in the bottlebrush polymer SEC traces indicate that termination by combination occurred during the RAFT step. This coupling product may be undetectable by SEC in the MM because it constitutes only a small amount of the sample, but it becomes apparent when synthesizing bottlebrush polymers.

Using the 20 MMs synthesized by RAFT, as detailed above, we prepared a total of 20 bottlebrush polymers using ROMP grafting-through initiated by Grubbs 3rd generation catalyst (G3) (**Scheme 3**). The nomenclature of these polymers follows the scheme $X_n^{y\%}$ where *X* is the MM type, *y*% is the targeted monomer conversion in the RAFT step, and *n* is the targeted number of MM repeating units in the bottlebrush polymer (N_{bb}) which was kept constant at 100. As noted above, all MM M_n values were near 3,000 g/mol, corresponding to N_{sc} values in the range of 16-27 for all MMs. As an example, $\mathbf{A}_{100}^{60\%}$ represents a bottlebrush PACMO with a target N_{bb} of 100 and 60% monomer conversion targeted in the RAFT step.

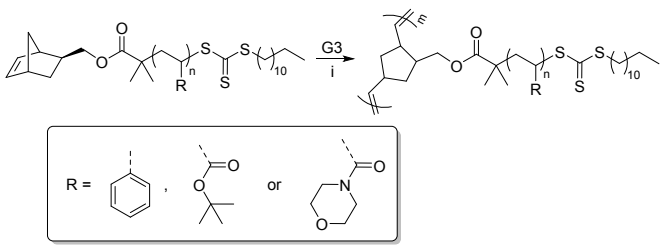

Scheme 3. Synthesis of PACMO bottlebrush polymers, P*t*BA bottlebrush polymers and PS bottlebrush polymers. Conditions: (i) CH_2Cl_2, rt, 1 h.

It is well-known that PS terminates by combination at a relatively high rate compared with other monomers, so our group and others typically target very low monomer conversions when preparing PS-MMs for bottlebrush polymer synthesis. At 10% MM to PS bottlebrush polymer conversion, there was no high molar mass shoulder in the RI or LS traces of the $\mathbf{S}_{\mathbf{100}}^{\mathbf{10\%}}$ bottlebrush polymer (**Figure 2**). However, for $\mathbf{S}_{\mathbf{100}}^{\mathbf{20\%}}$, the RI trace showed PS bottlebrush polymer with a noticeable high molar mass shoulder that was magnified in the LS trace to show the first observation of coupling. The greater intensity of the high molar mass shoulder in the LS trace results from the fact that the LS detector response depends on polymer molar mass while the RI detector response does not. Estimates at the peak of the shoulder showed that the molar mass of the shoulder peak was about twice the molar mass of the main peak, consistent with coupling products (Figures S9-S12). The area of the high molar mass shoulder increased with increasing monomer conversion levels in the PS-MMs. For $\mathbf{S}_{\mathbf{100}}^{\mathbf{50\%}}$ we observed a noticeable shift in the SEC peak toward lower elution time, consistent with the measured increase in the molar mass from around 270 kg/mol to 370 kg/mol (**Table 2**). Thus, enough coupling had occurred to the point where the overall molar mass of the PS bottlebrush polymer had increased. Peak deconvolution revealed about 14% coupling product (deconvolutions of the SEC traces for the PS bottlebrush polymers are shown in **Figures S39-S42**).

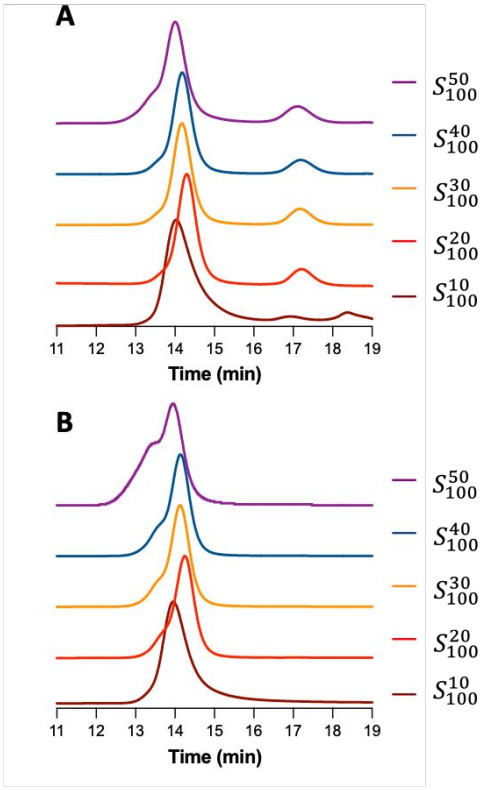

Figure 2. SEC traces showing (A) refractive index detector and (B) light scattering detector of PS bottlebrush polymers $\mathbf{S}_{\mathbf{100}}^{\mathbf{10\%}}$, $\mathbf{S}_{\mathbf{100}}^{\mathbf{20\%}}$, $\mathbf{S}_{\mathbf{100}}^{\mathbf{30\%}}$, $\mathbf{S}_{\mathbf{100}}^{\mathbf{40\%}}$ and $\mathbf{S}_{\mathbf{100}}^{\mathbf{50\%}}$.

Table 2. Molar masses by SEC for PS bottlebrush polymers.

Bottlebrush Polymer[a]	M_n[b] (kg/mol)	$Đ$[b]	% Conv.[c]	$P_{coupling}$[d]
$\mathbf{S}_{\mathbf{100}}^{\mathbf{10\%}}$	287	1.09	95	-
$\mathbf{S}_{\mathbf{100}}^{\mathbf{20\%}}$	266	1.10	95	4.0
$\mathbf{S}_{\mathbf{100}}^{\mathbf{30\%}}$	263	1.11	95	4.3
$\mathbf{S}_{\mathbf{100}}^{\mathbf{40\%}}$	264	1.12	95	5.7
$\mathbf{S}_{\mathbf{100}}^{\mathbf{50\%}}$	370	1.23	95	14

[a]Targeted bottlebrush polymer represented by $X_n^{y\%}$ where *X* is the MM type (S = PS), *y* is the targeted monomer conversion percentage for the MM in the RAFT polymerization, and *n* is the targeted number of MM repeating units in the bottlebrush polymer (N_{bb}). [b]For the entire peak as measured by SEC in THF at 30 °C using light scattering and refractive index detectors using d*n*/d*c* values noted in the Experimental Section. [c]Determined from SEC by comparing the integrations of the bottlebrush polymer peak and the MM peak. [d]Percentage of coupled bottlebrush polymers calculated using Equation 1 using the refractive index detector trace (Figures S39-S42).

The synthesis of P*t*BA bottlebrush polymers from P*t*BA-MMs also showed pronounced coupling but at higher MM to P*t*BA bottlebrush polymer conversions during RAFT polymerizations than in the PS bottlebrush polymers (**Scheme 3** and **Figure 3**). For MMs $\mathbf{T}^{\mathbf{50\%}}$,$\mathbf{T}^{\mathbf{60\%}}$ and $\mathbf{T}^{\mathbf{70\%}}$ no coupling was detected in the P*t*BA bottlebrush polymers of the ROMP reaction while maintaining dispersities below 1.20 (**Table 3**). These results suggest that the high molecular weight shoulders in these MMs, discussed above, are due to branching reactions in the MM synthesis. In the ROMP of MMs $\mathbf{T}^{\mathbf{80\%}}$, and $\mathbf{T}^{\mathbf{90\%}}$, a high molar mass shoulder became apparent in the RI traces and especially in the LS traces. Similar to PS-MMs, measurements at the peak

of the shoulders revealed that they were around twice as large as the main peak, which is consistent with coupling products (Figures S21 and S22). These results indicate that one should not exceed 70% conversion in the RAFT step in order to make well-defined P*t*BA bottlebrush polymers with N_{bb}=100; targeting a higher N_{bb} value would need even lower conversion in the RAFT step. Deconvolution of coupled bottlebrush polymer peaks in the RI spectra for BB polymers $\mathbf{T}_{100}^{80\%}$, and $\mathbf{T}_{100}^{90\%}$ conversions revealed 5.8% and 16% coupled product, respectively (**Figures S43 and S44**).

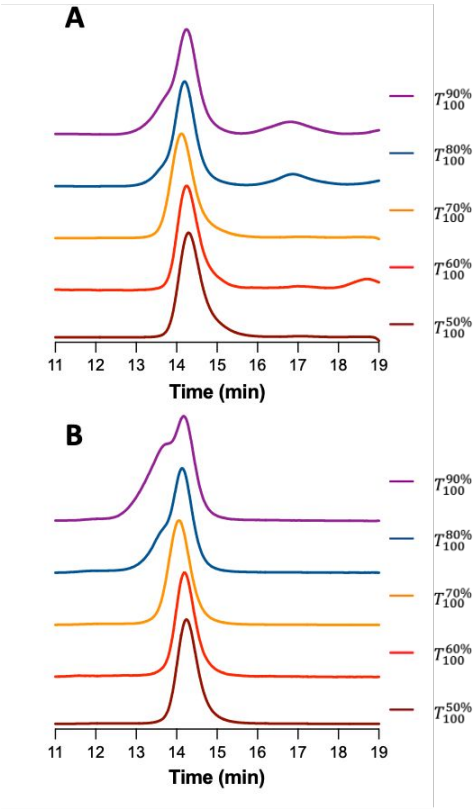

Figure 3. SEC traces showing (A) refractive index detector and (B) light scattering detector of P*t*BA bottlebrush polymers $\mathbf{T}_{100}^{50\%}$, $\mathbf{T}_{100}^{60\%}$, $\mathbf{T}_{100}^{70\%}$, $\mathbf{T}_{100}^{80\%}$ and $\mathbf{T}_{100}^{90\%}$.

Table 3. Molar masses by SEC for P*t*BA bottlebrush polymers.

Bottlebrush Polymer[a]	M_n[b] (kg/mol)	$Đ$[b]	% Conv.[c]	$P_{coupling}$[d]
$\mathbf{T}_{100}^{50\%}$	294	1.10	99	-
$\mathbf{T}_{100}^{60\%}$	322	1.07	94	-
$\mathbf{T}_{100}^{70\%}$	433	1.07	98	-
$\mathbf{T}_{100}^{80\%}$	390	1.18	85	5.8
$\mathbf{T}_{100}^{90\%}$	395	1.30	86	16

[a]Targeted bottlebrush polymer represented by $X_n^{y\%}$ where *X* is the MM type (T = P*t*BA), *y* is the targeted monomer conversion percentage for the MM in the RAFT polymerization, and *n* is the targeted number of MM repeating units in the bottlebrush polymer (N_{bb}). [b]For the entire peak as measured by SEC in THF at 30 °C using light scattering and refractive index detectors using d*n*/d*c* values noted in the Experimental Section. [c]Determined from SEC by comparing the integrations of the bottlebrush polymer peak and the MM peak. [d]Percentage of coupled bottlebrush polymers calculated using Equation 1 using the refractive index detector trace (Figures S43-S44).

The synthesis of PMMA bottlebrush polymers via grafting-through ROMP of MMs **M$^{50\%}$**, **M$^{60\%}$**, **M$^{70\%}$**, **M$^{80\%}$**, and **M$^{90\%}$** is shown in **Scheme 4**. Previously, Wooley and coworkers reported the synthesis of PMMA bottlebrush polymers through a one-pot synthesis approach because excess methyl methacrylate does not interfere with the ROMP reaction.[4] Still, we opted to purify the PMMA-MMs before synthesizing PMMA bottlebrush polymers by ROMP, as discussed above. While neither the RI nor the LS SEC traces showed a high molar mass shoulder, there was an increase in the dispersity of the PMMA bottlebrush polymers as the monomer conversion during the RAFT step increased (**Figure 4**). We attribute this increase in dispersity to termination by disproportionation, where residual alkenes on the chain ends can participate in the ROMP reaction, acting as chain terminators. Thus, targeting a monomer conversion of 50% during the synthesis of PMMA-MMs provided the most controlled polymerization to prepare PMMA bottlebrush polymers (**Table 4**).

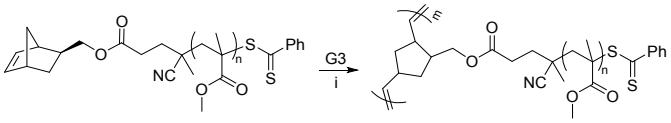

Scheme 4. Synthesis of PMMA bottlebrush polymers. Conditions: (i) CH_2Cl_2, rt, 1 h.

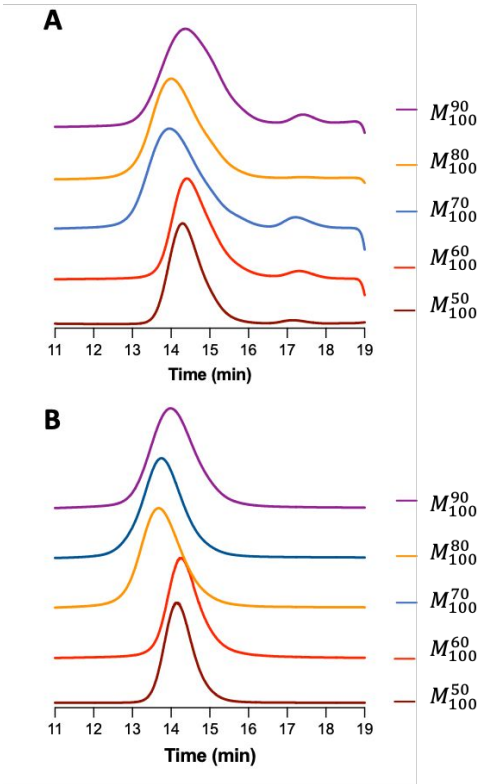

Figure 4. SEC traces showing (A) refractive index detector and (B) light scattering detector of PMMA bottlebrush polymers $\mathbf{M}_{100}^{50\%}$, $\mathbf{M}_{100}^{60\%}$, $\mathbf{M}_{100}^{70\%}$, $\mathbf{M}_{100}^{80\%}$ and $\mathbf{M}_{100}^{90\%}$.

Table 4. Molar masses by SEC for PMMA bottlebrush polymers.

Bottlebrush Polymer[a]	M_n[b] (kg/mol)	$Đ$[b]	% Conv.[c]
$\mathbf{M}_{100}^{50\%}$	259	1.23	98
$\mathbf{M}_{100}^{60\%}$	228	1.20	95
$\mathbf{M}_{100}^{70\%}$	365	1.41	94
$\mathbf{M}_{100}^{80\%}$	378	1.42	99
$\mathbf{M}_{100}^{90\%}$	263	1.35	92

[a]Targeted bottlebrush polymer represented by $X_n^{y\%}$ where *X* is the MM type (M = PMMA), *y* is the targeted monomer conversion percentage for the MM in the RAFT polymerization and *n* is the targeted number of MM repeating units in the bottlebrush polymer (N_{bb}). [b]For the entire peak as measured by SEC in THF at 30 °C using light scattering and refractive index detectors using d*n*/d*c* values noted in the Experimental Section. [c]Determined from SEC by comparing the integrations of the bottlebrush polymer peak and the MM peak.

For the synthesis of PACMO bottlebrush polymers, we targeted 50%, 60%, 70%, 80% and 90% monomer conversion by RAFT. Previously, we have reported the synthesis of PACMO bottlebrush polymers with a targeted monomer conversion of 80% with no detectable coupling.[44] As expected for this high k_p/k_t monomer, the synthesis of the PACMO bottlebrush polymers across all five MMs ($\mathbf{A}_{100}^{50\%}$, $\mathbf{A}_{100}^{60\%}$, $\mathbf{A}_{100}^{70\%}$, $\mathbf{A}_{100}^{80\%}$, and $\mathbf{A}_{100}^{90\%}$) showed no coupling either by RI or LS (**Figure 5**). Moreover, the M_n values were close to the targeted molar masses, and the dispersities did not exceed 1.20 (**Table 5**). These results demonstrate that growth-then-coupling for PACMO bottlebrush polymer is not necessarily advantageous compared with the direct-growth approach for avoiding the formation of bisnorbornenyl species.

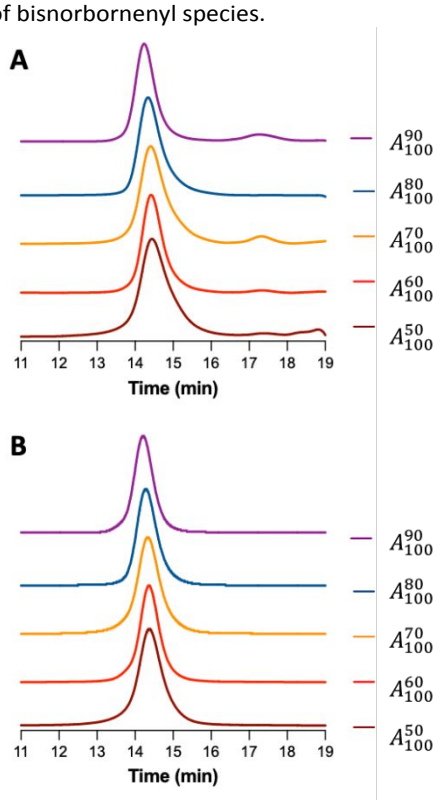

Figure 5. SEC traces showing (A) refractive index detector and (B) light scattering detector of PACMO bottlebrush polymers $\mathbf{A}_{100}^{50\%}$, $\mathbf{A}_{100}^{60\%}$, $\mathbf{A}_{100}^{70\%}$, $\mathbf{A}_{100}^{80\%}$ and $\mathbf{A}_{100}^{90\%}$.

Table 5. Molar masses by SEC for PACMO bottlebrush polymers.

Bottlebrush Polymer[a]	M_n[b] (kg/mol)	$Đ$[b]	% Conv.[c]
$\mathbf{A}_{100}^{50\%}$	267	1.08	97
$\mathbf{A}_{100}^{60\%}$	327	1.10	98
$\mathbf{A}_{100}^{70\%}$	306	1.13	94
$\mathbf{A}_{100}^{80\%}$	320	1.08	99
$\mathbf{A}_{100}^{90\%}$	472	1.04	89

[a]Targeted bottlebrush polymer represented by $X_n^{y\%}$ where *X* is the MM type (A = PACMO), *y* is the targeted monomer conversion percentage for the MM in the RAFT polymerization, and *n* is the targeted number of MM repeating units in the bottlebrush polymer (N_{bb}). [b]For the entire peak as measured by SEC in THF at 30 °C using light scattering and refractive index detectors using d*n*/d*c* values noted in the Experimental Section. [c]Determined from SEC by comparing the integrations of the bottlebrush polymer peak and the MM peak.

Taken together, the data show that there are two important aspects to consider in order to optimize bottlebrush polymer synthesis when synthesizing bottlebrush polymers utilizing the direct-growth approach. First, the potential to produce coupled bottlebrush polymers is determined by the tendency of the specific monomer to undergo radical-radical combination (coupling) reactions to generate bisnorbornenyl species. This is highlighted by the fact that the PACMO-MMs did not exhibit any sign of contamination with bisnorbornenyl species, as evidenced by consistently low dispersity values and no shoulders regardless of the monomer conversion percentage in the RAFT step. Second, the monomer conversion percentage within most monomer types significantly affects the quality of the bottlebrush polymers synthesized. This factor was particularly prevalent in the preparation of the PS and P*t*BA bottlebrush polymers, both of which showed no shoulders at low monomer conversion percentages (below 20% for PS-MMs and below 80% for P*t*BA-MMs), while coupling was detected for the higher conversions. In contrast, PMMA bottlebrush polymers showed a general increase in dispersity with increasing monomer conversion in the RAFT step, likely due to the formation of ROMP-active alkenes on the PMMA chain ends due to disproportionation.

Conclusion

In summary, we have investigated the tendency for four monomer types to produce bisnorbornenyl species during RAFT polymerization to generate MMs. To ensure no residual vinyl monomer in our samples, all MMs were purified by automated column chromatography on conventional silica instead of precipitations. This was a fast and effective method for purifying the MMs from unreacted monomers in a single step, limiting the use of excess solvents and unnecessary efforts during precipitations. In polymerization reactions converting MMs into bottlebrush polymers, we found that the direct-growth approach can be used to prepare well-defined, monomodal, and low *Đ* bottlebrush polymers using ROMP grafting-through.

The presence of even a trace of bisnorbornenyl species results in the formation of coupled bottlebrush polymers that can be observed by SEC analyses using RI and LS detectors. Furthermore, the type of monomer used, including styrenics, acrylates, methacrylates or acrylamides, dictates the limit for monomer conversion to MM in the RAFT or other RDRP step to limit termination reactions, in particular, termination by combination, which produces coupled bottlebrush polymers via the formation of bisnorbornenyl species. As a result, optimized bottlebrush syntheses using the direct growth approach can be accomplished, but one must consider monomer type and conversion percentage during the RDRP step to generate well-defined bottlebrush polymers without high molar mass shoulders.

Conflicts of interest

There are no conflicts to declare.

Acknowledgment

This work was supported by a joint grant between the National Science Foundation and the Binational Science Foundation (DMR-2104602). We thank Mrs. Sarah Swilley-Sanchez for helpful discussions regarding purifications.

References

1. R. Verduzco, X. Li, S. L. Pesek and G. E. Stein, *Chem. Soc. Rev.*, 2015, **44**, 2405-2420.
2. J. C. Foster, S. C. Radzinski and J. B. Matson, *J. Polym. Sci., Part A: Polym. Chem.*, 2017, **55**, 2865-2876.
3. Z. Li, M. Tang, S. Liang, M. Zhang, G. M. Biesold, Y. He, S.-M. Hao, W. Choi, Y. Liu, J. Peng and Z. Lin, *Prog. Polym. Sci.*, 2021, **116**, 101387.
4. A. Li, J. Ma, G. Sun, Z. Li, S. Cho, C. Clark and K. L. Wooley, *J. Polym. Sci., Part A: Polym. Chem.*, 2012, **50**, 1681-1688.
5. W. J. Neary, B. A. Fultz and J. G. Kennemur, *ACS Macro Lett.*, 2018, **7**, 1080-1086.
6. M. Alaboalirat and J. B. Matson, *ACS Macro Lett.*, 2021, **10**, 1460-1466.
7. J. Choi, H. Kim, T. Do, J. Moon, Y. Choe, J. G. Kim and J. Bang, *J. Polym. Sci., Part A: Polym. Chem.*, 2019, **57**, 726-737.
8. C. Lexer, R. Saf and C. Slugovc, *J. Polym. Sci., Part A: Polym. Chem.*, 2009, **47**, 299-305.
9. Y. C. Teo and Y. Xia, *Macromolecules*, 2015, **48**, 5656-5662.
10. C. Cheng, E. Khoshdel and K. L. Wooley, *Macromolecules*, 2005, **38**, 9455-9465.
11. D. L. Patton and R. C. Advincula, *Macromolecules*, 2006, **39**, 8674-8683.
12. M. Naguib, K. L. Nixon and D. J. Keddie, *Polym. Chem.*, 2022, **13**, 1401-1410.
13. B. R. Clarke and G. N. Tew, *J. Polym. Sci.*, 2022, **60**, 1501-1510.
14. W. Hou, Z. Li, L. Xu, Y. Li, Y. Shi and Y. Chen, *ACS Macro Lett.*, 2021, **10**, 1260-1265.
15. D. J. Walsh, S. Dutta, C. E. Sing and D. Guironnet, *Macromolecules*, 2019, **52**, 4847-4857.
16. D. J. Walsh and D. Guironnet, *Proc. Natl. Acad. Sci. U.S.A.*, 2019, DOI: 10.1073/pnas.1817745116, 201817745.
17. S. E. Blosch, M. Alaboalirat, C. B. Eades, S. J. Scannelli and J. B. Matson, *Macromolecules*, 2022, **55**, 3522-3532.
18. S. E. Blosch, S. J. Scannelli, M. Alaboalirat and J. B. Matson, *Macromolecules*, 2022, **55**, 4200-4227.
19. N. B. Sankaran, A. Z. Rys, R. Nassif, M. K. Nayak, K. Metera, B. Chen, H. S. Bazzi and H. F. Sleiman, *Macromolecules*, 2010, **43**, 5530-5537.
20. M. F. Fouz, K. Mukumoto, S. Averick, O. Molinar, B. M. McCartney, K. Matyjaszewski, B. A. Armitage and S. R. Das, *ACS Cent. Sci.*, 2015, **1**, 431-438.
21. M. A. Sowers, J. R. McCombs, Y. Wang, J. T. Paletta, S. W. Morton, E. C. Dreaden, M. D. Boska, M. F. Ottaviani, P. T. Hammond, A. Rajca and J. A. Johnson, *Nat. Commun.*, 2014, **5**, 5460.
22. P. Zhao, L. Liu, X. Feng, C. Wang, X. Shuai and Y. Chen, *Macromol. Rapid Commun.*, 2012, **33**, 1351-1355.
23. J. A. Johnson, Y. Y. Lu, A. O. Burts, Y. Xia, A. C. Durrell, D. A. Tirrell and R. H. Grubbs, *Macromolecules*, 2010, **43**, 10326-10335.
24. C. R. Powell, K. Kaur, K. M. Dillon, M. Zhou, M. Alaboalirat and J. B. Matson, *ACS Chem. Bio.*, 2019, **14**, 1129-1134.
25. P. Ramamurthi, Z. Zhao, E. Burke, N. F. Steinmetz and M. Müllner, *Advanced Healthcare Materials*, 2022, 2200163.
26. T. Pelras, C. S. Mahon, Nonappa, O. Ikkala, A. H. Gröschel and M. Müllner, *J. Am. Chem. Soc.*, 2018, **140**, 12736-12740.
27. C. M. Tonge, E. R. Sauvé, S. Cheng, T. A. Howard and Z. M. Hudson, *J. Am. Chem. Soc.*, 2018, **140**, 11599-11603.
28. W. F. M. Daniel, J. Burdynska, M. Vatankhah-Varnoosfaderani, K. Matyjaszewski, J. Paturej, M. Rubinstein, A. V. Dobrynin and S. S. Sheiko, *Nat Mater*, 2016, **15**, 183-189.
29. L.-H. Cai, T. E. Kodger, R. E. Guerra, A. F. Pegoraro, M. Rubinstein and D. A. Weitz, *Adv. Mater.*, 2015, **27**, 5132-5140.
30. J. M. Sarapas, E. P. Chan, E. M. Rettner and K. L. Beers, *Macromolecules*, 2018, **51**, 2359-2366.
31. V. G. Reynolds, S. Mukherjee, R. Xie, A. E. Levi, A. Atassi, T. Uchiyama, H. Wang, M. L. Chabinyc and C. M. Bates, *Mater. Horiz.*, 2020, **7**, 181-187.
32. C. Clair, A. Lallam, M. Rosenthal, M. Sztucki, M. Vatankhah-Varnosfaderani, A. N. Keith, Y. Cong, H. Liang, A. V. Dobrynin, S. S. Sheiko and D. A. Ivanov, *ACS Macro Lett.*, 2019, **8**, 530-534.
33. B. R. Sveinbjörnsson, R. A. Weitekamp, G. M. Miyake, Y. Xia, H. A. Atwater and R. H. Grubbs, *Proc. Natl. Acad. Sci. U.S.A.*, 2012, **109**, 14332-14336.
34. R. J. Macfarlane, B. Kim, B. Lee, R. A. Weitekamp, C. M. Bates, S. F. Lee, A. B. Chang, K. T. Delaney, G. H. Fredrickson, H. A. Atwater and R. H. Grubbs, *J. Am. Chem. Soc.*, 2014, **136**, 17374-17377.
35. G. M. Miyake, V. A. Piunova, R. A. Weitekamp and R. H. Grubbs, *Angew. Chem. Int. Ed.*, 2012, **51**, 11246-11248.
36. Y.-G. Yu, C. Seo, C.-G. Chae, H.-B. Seo, M.-J. Kim, Y. Kang and J.-S. Lee, *Macromolecules*, 2019, **52**, 4349-4358.
37. D.-P. Song, T. H. Zhao, G. Guidetti, S. Vignolini and R. M. Parker, *ACS Nano*, 2019, **13**, 1764-1771.
38. Y.-L. Li, X. Chen, H.-K. Geng, Y. Dong, B. Wang, Z. Ma, L. Pan, G.-Q. Ma, D.-P. Song and Y.-S. Li, *Angew. Chem. Int. Ed.*, 2021, **60**, 3647-3653.
39. E. Altay, D. Nykypanchuk and J. Rzayev, *ACS Nano*, 2017, **11**, 8207-8214.
40. X. Chen, X. Yang, D.-P. Song, Y.-F. Men and Y. Li, *Macromolecules*, 2021, **54**, 3668-3677.
41. H.-F. Fei, W. Li, A. Bhardwaj, S. Nuguri, A. Ribbe and J. J. Watkins, *J. Am. Chem. Soc.*, 2019, **141**, 17006-17014.
42. Y. Xia, J. A. Kornfield and R. H. Grubbs, *Macromolecules*, 2009, **42**, 3761-3766.

43. Z. Li, K. Zhang, J. Ma, C. Cheng and K. L. Wooley, *J. Polym. Sci., Part A: Polym. Chem.*, 2009, **47**, 5557-5563.
44. M. Alaboalirat, L. Qi, K. J. Arrington, S. Qian, J. K. Keum, H. Mei, K. C. Littrell, B. G. Sumpter, J.-M. Y. Carrillo and R. Verduzco, *Macromolecules*, 2018, **52**, 465-476.
45. S. Onbulak and J. Rzayev, *J. Polym. Sci., Part A: Polym. Chem.*, 2017, **55**, 3868-3874.
46. J. Nam, Y. Kim, J. G. Kim and M. Seo, *Macromolecules*, 2019, **52**, 9484-9494.
47. X. Li, H. ShamsiJazeyi, S. L. Pesek, A. Agrawal, B. Hammouda and R. Verduzco, *Soft Matter*, 2014, **10**, 2008-2015.
48. B. R. Sveinbjörnsson, R. A. Weitekamp, G. M. Miyake, Y. Xia, H. A. Atwater and R. H. Grubbs, *Proc. Natl. Acad. Sci. U.S.A.*, 2012, **109**, 14332.
49. M. Naguib, K. L. Nixon and D. J. Keddie, *Polym. Chem.*, 2022.
50. J. A. Love, J. P. Morgan, T. M. Trnka and R. H. Grubbs, *Angew. Chem. Int. Ed.*, 2002, **41**, 4035-4037.
51. J. Liu, A. X. Gao and J. A. Johnson, *J. Vis. Exp.*, 2013, DOI: doi:10.3791/50874, e50874.
52. S. Mori and H. G. Barth, *Size exclusion chromatography*, Springer Science & Business Media, 1999.
53. E. Kurnaz, E. Helvacioglu, N. C. Kekec, N. Nugay, T. Nugay and J. P. Kennedy, *J. Polym. Sci., Part A: Polym. Chem.*, 2019, **57**, 1197-1208.
54. W. G. Weber, J. B. McLeary and R. D. Sanderson, *Tetrahedron Lett.*, 2006, **47**, 4771-4774.
55. M. Benaglia, E. Rizzardo, A. Alberti and M. Guerra, *Macromolecules*, 2005, **38**, 3129-3140.
56. Y.-S. Ye, W.-C. Shen, C.-Y. Tseng, J. Rick, Y.-J. Huang, F.-C. Chang and B.-J. Hwang, *Chem. Commun.*, 2011, **47**, 10656-10658.
57. M. Alaboalirat, L. Qi, K. J. Arrington, S. Qian, J. K. Keum, H. Mei, K. C. Littrell, B. G. Sumpter, J.-M. Y. Carrillo, R. Verduzco and J. B. Matson, *Macromolecules*, 2019, **52**, 465-476.
58. S. C. Radzinski, J. C. Foster, R. C. Chapleski, D. Troya and J. B. Matson, *J. Am. Chem. Soc.*, 2016, **138**, 6998-7004.
59. V. Schreck, A. Serelis and D. Solomon, *Aust. J. Chem.*, 1989, **42**, 375-393.
60. Y. Nakamura and S. Yamago, *Macromolecules*, 2015, **48**, 6450-6456.
61. K. Antolin, J.-P. Lamps, P. Rempp and Y. Gnanou, *Polymer*, 1990, **31**, 967-970.
62. K. G. Bradford, L. M. Petit, R. Whitfield, A. Anastasaki, C. Barner-Kowollik and D. Konkolewicz, *J. Am. Chem. Soc.*, 2021, **143**, 17769-17777.
63. D. Konkolewicz, S. Sosnowski, D. R. D'hooge, R. Szymanski, M.-F. Reyniers, G. B. Marin and K. Matyjaszewski, *Macromolecules*, 2011, **44**, 8361-8373.
64. A. K. Chatterjee, T.-L. Choi, D. P. Sanders and R. H. Grubbs, *J. Am. Chem. Soc.*, 2003, **125**, 11360-11370.